

Rapid Simulation of Irradiation Damage in PWR Internals NSUF Milestone Report



Miao Song
Jesse Werden
Kory Linton
Kevin G. Field
Gary S. Was

January 2020

DOCUMENT AVAILABILITY

Reports produced after January 1, 1996, are generally available free via US Department of Energy (DOE) SciTech Connect.

Website <http://www.osti.gov>

Reports produced before January 1, 1996, may be purchased by members of the public from the following source:

National Technical Information Service
5285 Port Royal Road
Springfield, VA 22161
Telephone 703-605-6000 (1-800-553-6847)
TDD 703-487-4639
Fax 703-605-6900
E-mail info@ntis.gov
Website <http://classic.ntis.gov/>

Reports are available to DOE employees, DOE contractors, Energy Technology Data Exchange representatives, and International Nuclear Information System representatives from the following source:

Office of Scientific and Technical Information
PO Box 62
Oak Ridge, TN 37831
Telephone 865-576-8401
Fax 865-576-5728
E-mail reports@osti.gov
Website <http://www.osti.gov/contact.html>

This report was prepared as an account of work sponsored by an agency of the United States Government. Neither the United States Government nor any agency thereof, nor any of their employees, makes any warranty, express or implied, or assumes any legal liability or responsibility for the accuracy, completeness, or usefulness of any information, apparatus, product, or process disclosed, or represents that its use would not infringe privately owned rights. Reference herein to any specific commercial product, process, or service by trade name, trademark, manufacturer, or otherwise, does not necessarily constitute or imply its endorsement, recommendation, or favoring by the United States Government or any agency thereof. The views and opinions of authors expressed herein do not necessarily state or reflect those of the United States Government or any agency thereof.

Reactor and Nuclear Systems Division

**RAPID SIMULATION OF IRRADIATION DAMAGE IN PWR INTERNALS
NSUF MILESTONE REPORT**

Miao Song
Jesse Werden
Kory Linton
Kevin G. Field
Gary S. Was

Date Published: January 2020

NSUF Work Package #: UF-20OR021108
Work Package Manager: Kory Linton
Milestone #: M3UF-20OR0211082

Prepared by
OAK RIDGE NATIONAL LABORATORY
Oak Ridge, TN 37831-6283
managed by
UT-BATTELLE, LLC
for the
US DEPARTMENT OF ENERGY
under contract DE-AC05-00OR22725

CONTENTS

LIST OF FIGURES.....	v
LIST OF TABLES	v
ACRONYMs.....	vii
ACKNOWLEDGMENTS	ix
EXECUTIVE SUMMARY	xi
1. INTRODUCTION.....	1
2. SUMMARY OF WORK COMPLETED.....	1
3. SPECIMEN PREPARATION.....	2
3.1 RECEIPT OF SAMPLES.....	2
3.2 PREPARATION OF TEM LAMELLAE.....	2
3.3 PREPARATION OF APT SPECIMENS	3
4. RESULTS	3
4.1 ZERO DPA SAMPLE.....	3
4.2 NEUTRON-IRRADIATED SAMPLES	4
4.3 NEUTRON + ION IRRADIATED SAMPLES.....	5
5. CONCLUSIONS AND FUTURE WORK	8

LIST OF FIGURES

Figure 1. Dislocation and twinning microstructure apparent in the zero dpa sample.....	3
Figure 2: Nanocavities observed in different neutron-irradiated samples with nominal doses of (a) 41, (b) 74, and (c) 100 dpa.	4
Figure 3: Frank loops observed in different neutron irradiated samples with nominal doses of (a) 41, (b) 74, and (c) 100 dpa.	4
Figure 4: Atom maps for the neutron-irradiated specimens to different damage levels.....	5
Figure 5: Microstructural features in neutron (38 dpa) + ion-irradiated (34 dpa) samples.	6
Figure 6: Clusters in neutron + ion (a) 390°C and (b) 410°C, and (c) neutron irradiated samples to similar dose, ~73dpa.	6
Figure 7: A direct comparison of feature size and density in neutron and neutron + ion irradiated samples with a similar damage level ~73dpa. (a) feature size and (b) feature density. The temperature of neutron + ion irradiation indicates the experimental temperature of ion irradiation.	7
Figure 8: Radiation-induced segregation in neutron- and neutron + ion irradiated samples.	7
Figure 9: A direct comparison of RIS in neutron and neutron + ion irradiated samples with a similar damage level ~73dpa. (a) Major elements and (b) Minor elements. The temperature of neutron + ion irradiation indicates the experimental temperature of ion irradiation.	8

LIST OF TABLES

Table 1. Summary of microstructural characterization activity.....	1
Table 2. Chemical composition (wt %) of 316 stainless steel for manufacturing flux thimble tubes.	2
Table 3. Reactor irradiated conditions of the samples sectioned from FTT-100.	2

ACRONYMS

APT	atom probe tomography
DOE	US Department of Energy
EDS	energy-dispersive spectroscopy
FIB	focused ion beam
LAMDA	Low Activation Materials Development and Analysis
MC ²	the University of Michigan Center for Materials Characterization
NSUF	Nuclear Science User Facility
ORNL	Oak Ridge National Laboratory
PWR	pressurized water reactor
RIS	radiation-induced segregation
STEM	scanning/transmission electron microscope (microscopy)
TEM	transmission electron microscope (microscopy)
UM	the University of Michigan

ACKNOWLEDGMENTS

This research used resources at the Low Activation Materials Design and Analysis laboratory operated by the Oak Ridge National Laboratory. Funding for this research was provided by the US Department of Energy Office of Nuclear Energy Nuclear Science User Facilities Consolidated Innovative Nuclear Research program. This report was authored by UT-Battelle LLC under Contract No. DE-AC05-00OR22725 with the US Department of Energy.

EXECUTIVE SUMMARY

This document summarizes the progress made by Oak Ridge National Laboratory (ORNL) in collaboration with the University of Michigan on “Rapid Simulation of Irradiation Damage in PWR Internals,” a research project led by the University of Michigan and supported by US Department of Energy Office of Nuclear Energy Nuclear Science User Facilities Consolidated Innovative Nuclear Research program. In this reporting period, samples that were exposed to combined neutron and ion irradiation were prepared and shipped to the University of Michigan for further analysis. This report summarizes the specimen preparation performed at ORNL’s Low Activation Materials Development and Analysis facility. The benchmarking work of microstructural characterization on reactor-irradiated samples with different dose levels was completed.

1. INTRODUCTION

The objective of this study is to demonstrate that self-ion irradiation after reactor irradiation can simulate microstructural damage produced solely by reactor irradiation. To meet this objective, specimens that have experienced reactor-irradiation conditions only and specimens that have experienced reactor+self-ion-irradiation conditions will be examined for microstructural features such as dislocation loops, cavities/voids, Ni-Si clusters, and radiation-induced segregation (RIS), and the features will be characterized. The Electric Power Research Institute provided the base material for the two types of specimens. The characterization of the microstructures will require the application of a range of techniques, which are to be completed at Oak Ridge National Laboratory's (ORNL's) Low Activation Materials Development and Analysis (LAMDA) facility. The analytical techniques include scanning transmission electron microscopy (STEM), X-ray energy-dispersive spectroscopy (EDS), atom probe tomography (APT), Fresnel-contrast imaging, and rel-rod-based diffraction imaging using transmission electron microscopy (TEM). This report summarizes the progress of this ongoing project.

2. SUMMARY OF WORK COMPLETED

A summary of the work completed is provided in Table 1. Only the characterization efforts are captured, but additional shipments between the University of Michigan and ORNL were made to complete the efforts. Table 1 shows that a total of 23 TEM lift-outs and 8 APT lift-outs (~5 tips/lift-out) have been completed to date. These efforts have enabled a full characterization of the neutron-irradiated specimens as well as extensive characterization of samples that have been neutron-irradiated and then have undergone the additional ion irradiations. Characterization was completed using a systematic approach that uses both the LAMDA capabilities at the ORNL Nuclear Science User Facility, including the FEI Talos F200X, and the University of Michigan's Michigan Center for Materials Characterization (MC²). Sample preparation and characterization activities are summarized in the following sections.

Table 1. Summary of microstructural characterization activity.

Sample ID*	dpa (particle)	Sample count				In UM
		TEM lift-outs	RISs	Mapping of PPTs	APT (tips)	
K2A2+3-4_N0	0	2	2	1	0	Yes
D3B4-3_N74_312	74 (n)	2	4	1	10	Yes
G7K11A6-1_N75_323	76 (n)	2	4	2	10	Yes
K2A2+3-1_N0_I38_390	38 (Ni ³⁺)	4	0	0	0	Yes
K2A2+3-2_N0_I38_410	38 (Ni ³⁺)	3	1	1	0	Yes
D3A2-1_N41_300	41(n)	3	2	2	10	Yes
D3A1-1_N38_I34_410	72 (n+Ni ³⁺)	2	3	2	0	Yes
D3A1-2_N38_I34_390	72 (n+Ni ³⁺)	3	2	2	0	Yes
D3A1-1_N38_I34_I28_410	100 (n+Ni ³⁺)	0	0	0	0	No
D3C4-3_N100_323	100 (n)	2	1	0	10	Yes

*Note: The sample ID includes sample information. For example, in D3A1-1_N38_I34_410, D3A1-1 indicates the location where the sample was taken from the flux thimble tube, N38 indicates the neutron irradiated dose, I34 indicates the ion irradiation dose, and 410 indicates the ion irradiation temperature.

3. SPECIMEN PREPARATION

3.1 RECEIPT OF SAMPLES

Two flux thimble tubes from the commercial Ringhals Pressurized Water Reactor (PWR) Unit 2 were obtained for this study. The chemical composition is provided in Table 2. The tubes had undergone either 29 or 34 reactor cycles, resulting in a peak dose of 76 displacements per atom (dpa) and 100 dpa, respectively. Due to the axial damage gradient in the core of the Ringhals PWR, the minimum dose was essentially zero at the limiting ends of the flux thimble tubes. Thus, a series of power reactor-irradiated specimens with nominally similar temperatures but varying doses could be obtained. Table 3 lists the parent flux thimble tube identification, the nominal damage doses, and temperatures to the best of our knowledge.

Table 2. Chemical composition (wt %) of 316 stainless steel for manufacturing flux thimble tubes.

Material	C	Mn	P	S	Si	Cr	Mo	Ni	Co	Fe
316SS	0.045	1.7	0.026	0.01	0.43	17.4	2.69	13.3	0.04	Bal.

Table 3. Reactor irradiated conditions of the samples sectioned from FTT-100.

Tube ID	Dose (dpa)	Damage rate ($\times 10^{-8}$ dpa/s)	Temperature (°C)
FTT-76	~0	-	~285
FTT-100	~41	5.53	~300
FTT-100	~74	9.98	~312
FTT-100	100	13.5	~323

The samples listed in Table 3 were shipped to ORNL for microscopic investigations. The samples, in the form of 3 mm discs, were received in the Irradiated Materials Examination and Testing hot cell facility. Remote operation was conducted to verify the samples and to prepare them for shipment to the Low Activation Materials Design and Analysis (LAMDA) laboratory. Following verification of the bulk samples, a shipment containing all of the samples was made to LAMDA.

In FY 2018, a series of bulk, 3 mm disc reactor-irradiated sister samples were shipped to the University of Michigan to complete the ion irradiation additions on the lower-dose specimens to emulate the higher-dose reactor-irradiated specimens. Throughout FY 2019, the reactor-+ion-irradiated samples were shipped back to LAMDA to perform additional microscopy and characterization in the same manner as the original reactor-irradiated specimens.

3.2 PREPARATION OF TEM LAMELLAE

Samples for TEM, STEM, and APT were prepared using the standard focus ion beam (FIB) technique in an FEI Versa 3D FIB/SEM dualbeam. This step is essential for handling the specimens. The small volume of a FIB lift-out yields a specimen with a low activity, just slightly above the background value as compared to the parent sample, which emits high levels of radioactivity. The reduced sample activity enabled rapid characterization of the samples in LAMDA microscopes and/or shipment to the University of Michigan for further characterization.

TEM samples were first investigated at ORNL in the LAMDA facility using the FEI F200X Talos S/TEM. The Talos S/TEM provided for efficient EDS mapping of regions of interest. STEM-EDS was

employed to evaluate the degree of RIS to random high-angle grain boundaries. Grain boundaries were tilted to the edge-on condition with the grain boundary oriented vertically in each region of interest. Mapping was completed using a 1 h total scan time and a pixel size of $1,024 \times 1,024$ with drift correction. After the STEM-EDS maps were collected, the maps were converted to 1D line scans across the grain boundaries by binning parallel to the axis of the grain boundary. Binning helped the signal-to-noise ratio and enabled determination of the relative amounts of elements segregating to the grain boundaries.

3.3 PREPARATION OF APT SPECIMENS

APT specimens in the form of dulled tips were pulled from a general location near the center of each specimen following standard FIB-based lift-out methods. The first step of annular milling was performed on each APT tip to reduce the volume of material so that the sample activity was below background limits for shipping. The APT tips were then determined to be below background limits for radioactive samples, enabling preparation and shipment of samples to MC² at the University of Michigan. Table 2 lists the number of APT tips per sample that were created in LAMDA for this project.

The APT tips were evaporated using the laser mode of a Cameca LEAP 5000XHR APT system with 40 pJ laser energy at 40 K and a detection rate of 0.5%. Five samples were run at each damage level, but only the largest two data sets were analyzed further. Reconstruction of the relative atom position was conducted using the IVAS 3.8.2. As the actual shapes of the tips were unknown; the compression factor and evaporate field were set as default values, which are about 1.65 and 33 V/nm, respectively.

4. RESULTS

4.1 ZERO DPA SAMPLE

The zero dpa sample (K2A2+3-4_N0, Table 1) was evaluated to determine whether some irradiation damage occurred to specimens in the furthest axial positions in the power reactor. The estimated damage level was ~ 0.002 dpa, which in austenitic stainless steels is well below the saturation regime for microstructural evolution at typical reactor irradiation temperatures. The general microstructural observations using TEM confirmed these assumptions. No damage was found in the forms of loops, precipitation, or RIS to grain boundaries. The material contained a typical cold-work structure with deformation twins also apparent (Figure 1).

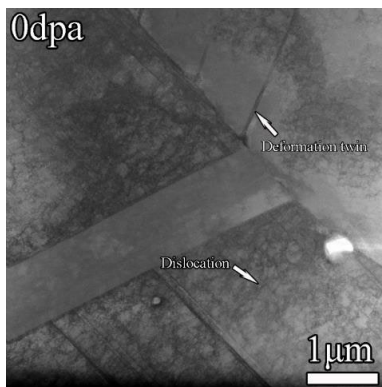


Figure 1. Dislocation and twinning microstructure apparent in the zero dpa sample.

4.2 NEUTRON-IRRADIATED SAMPLES

The neutron-irradiated samples showed microstructures consistent with neutron irradiation, including dislocation loops, nanocavities, and Ni-Si-rich clusters (Figures 2–4). The nanocavity population was found to be homogenously distributed in all three irradiation conditions (41, 71, and 100 dpa). It is assumed that the nanocavities are indeed bubbles that contain He from the transmutation reaction between the irradiating neutrons and the alloy composition. Bubbles were observed to be smaller than 3 nm with the mean size hovering near 1 nm in diameter. The density in all conditions was found to be near 10^{23} m^{-3} . The changes in size and number density were insignificant with dose, suggesting that cavity microstructure had saturated by 41 dpa in the flux thimble tube specimens.

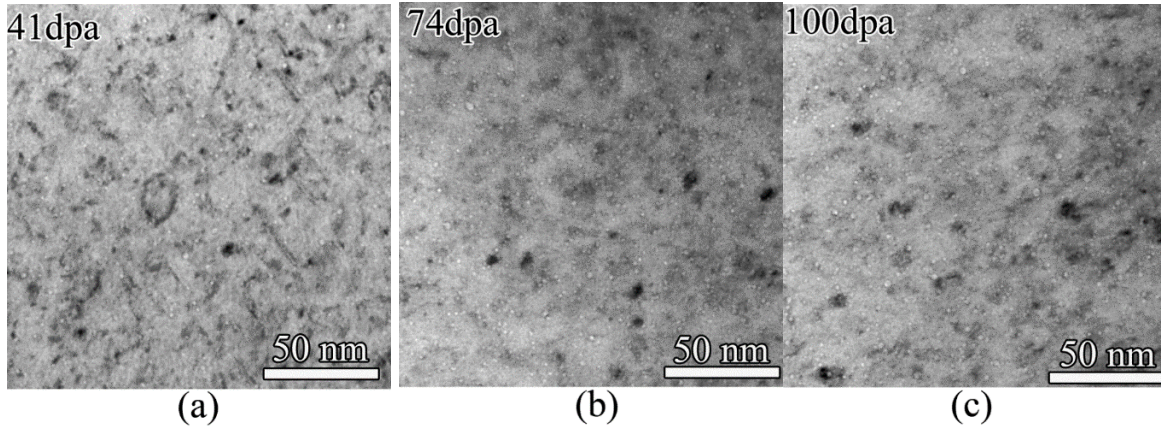


Figure 2: Nanocavities observed in different neutron-irradiated samples with nominal doses of (a) 41, (b) 74, and (c) 100 dpa. All the images were taken with an underfocus of 512 nm.

Frank loops were observed in all three doses, as shown in Figure 3. The average loop sizes were about 10 nm, and the number density ranged from 3.5×10^{22} to $4.7 \times 10^{22} \text{ m}^{-2}$. The size distribution appeared to be log-normal with a tail toward larger loops. The dose-dependent size or number density was insignificant, which indicates a saturation of loops.

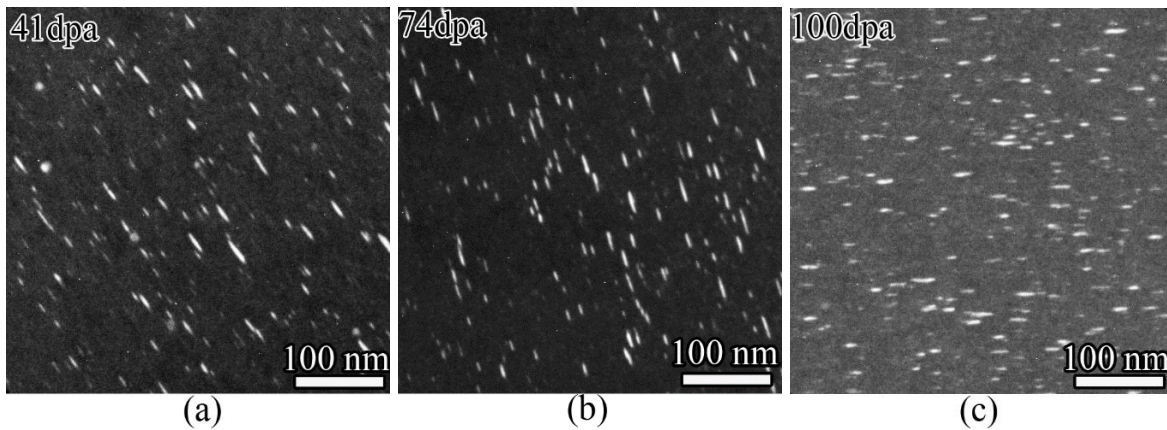


Figure 3: Frank loops observed in different neutron irradiated samples with nominal doses of (a) 41, (b) 74, and (c) 100 dpa.

STEM-EDS and APT revealed the formation of Ni-Si clusters. Atom maps from the atom probe data sets are provided in Figure 4. (Only the atom maps are shown here for brevity). Quantitative composition analysis indicated that Ni continued to enrich in the Ni-Si clusters with increasing dose. The 100 dpa samples have a chemistry consistent with Ni_3Si , which would indicate γ' precipitates. TEM was performed to further confirm the nature of the clusters observed in TEM and in STEM, but no diffraction spots were observed, which is potentially consistent with γ' precipitates. STEM-EDS also revealed the presence of RIS in the microstructure; Fe, Cr, and Mo were depleted, and Ni, Si, and P were enriched at the grain boundaries. The segregations of Fe and Ni in the 41 dpa samples were consistent with those in the 100 dpa specimen; the segregations of Fe and Ni in the 74 dpa samples were inconsistent with either of the other two doses.

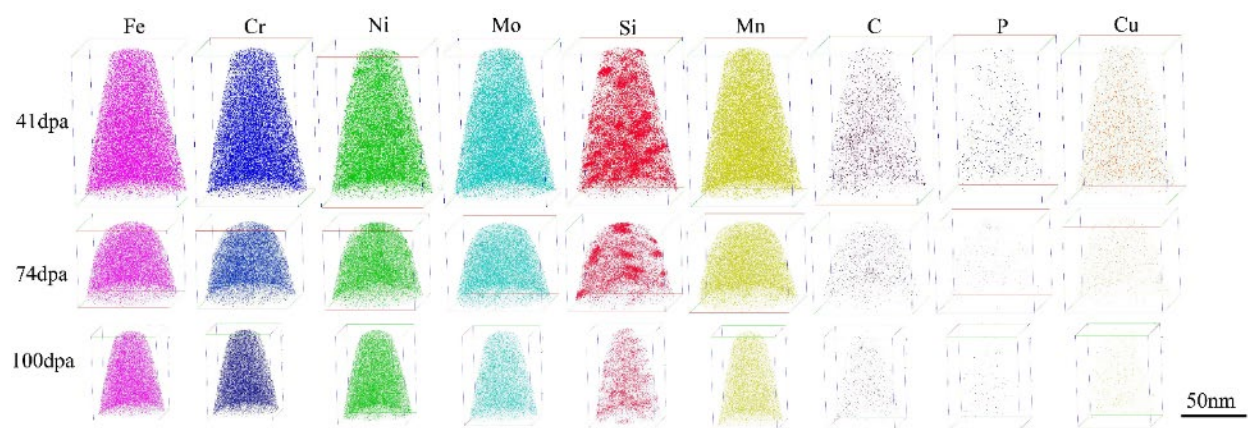


Figure 4: Atom maps for the neutron-irradiated specimens to different damage levels.

4.3 NEUTRON + ION IRRADIATED SAMPLES

Ion irradiations were performed at 390°C and 410°C to add 34 dpa on the 38 dpa reactor-irradiated samples. Each sample had a total dose of 72 dpa and was directly compared with a reactor-irradiated sample at a similar condition (74 dpa). Figure 5 shows the nanocavities and dislocation loops in the neutron + ion irradiated samples. A direct comparison of the Ni-Si clusters in neutron and neutron + ion irradiated samples is shown in Figure 6. The nanocavities, dislocation loops, and Ni-Si-rich clusters were very consistent between neutron and neutron- + ion-irradiated conditions as shown in Figure 7. RIS was measured by STEM EDX, which later converted to 1D line scans across the grain boundaries. The Modified inverse Kirkendall model was applied to predict the RIS with neutron irradiation condition. RIS results indicated that irradiation at 410°C seems a better condition because the major elements match well with the trend of reactor radiation conditions, as shown in Figure 8 and Figure 9. RIS of Mo in both ion-irradiation conditions failed to reproduce the trend of reactor radiation conditions. RIS of Si was confusing; ion irradiation at 390°C matched well with 100 dpa reactor-irradiated samples, whereas ion irradiation at 410°C agreed with the 41 dpa reactor-irradiated samples. However, none was consistent with the 74 dpa reactor-irradiated samples.

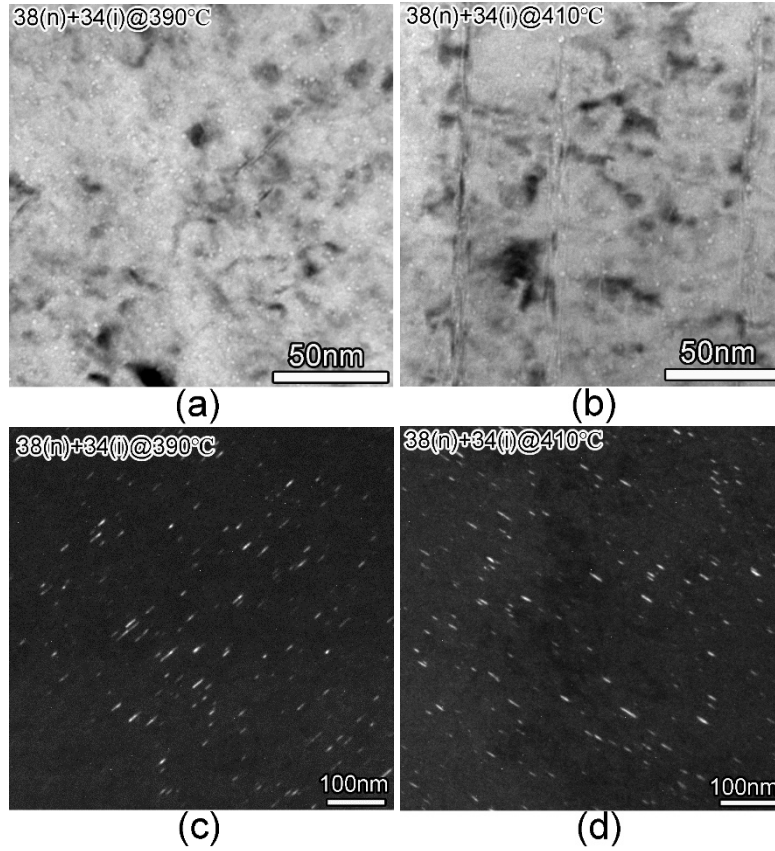


Figure 5: Microstructural features in neutron (38 dpa) + ion-irradiated (34 dpa) samples. Nanocavities in samples with an ion-irradiation temperature of (a) 390°C and (b) 410°C. Dislocation loops in samples with an ion irradiation temperature of (c) 390°C and (d) 410°C.

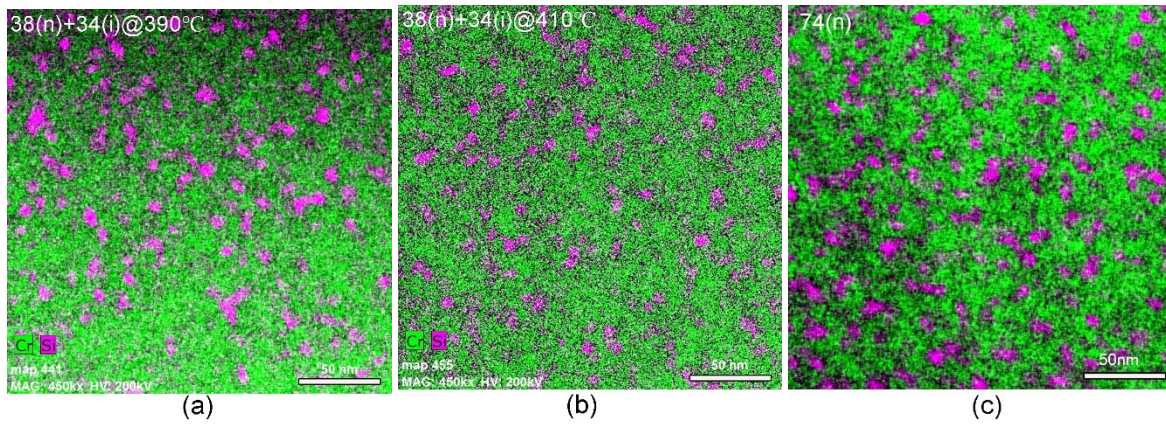


Figure 6: Clusters in neutron + ion (a) 390°C and (b) 410°C, and (c) neutron irradiated samples to similar dose, ~73dpa.

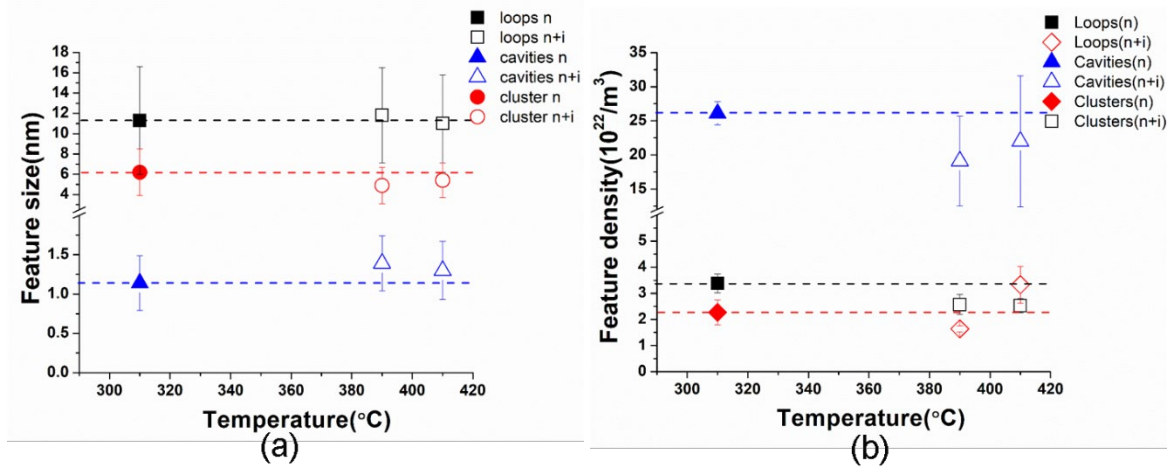


Figure 7: A direct comparison of feature size and density in neutron and neutron + ion irradiated samples with a similar damage level ~ 73 dpa. (a) feature size and (b) feature density. The temperature of neutron + ion irradiation indicates the experimental temperature of ion irradiation.

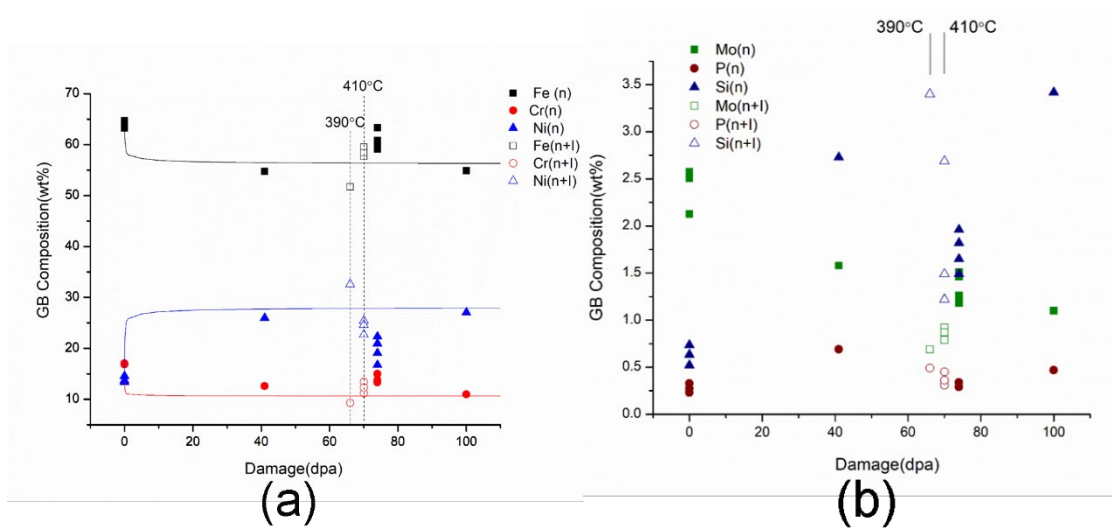


Figure 8: Radiation-induced segregation in neutron- and neutron + ion irradiated samples. Grain boundary composition: (a) major elements and (b) minor elements. The dpa levels were offset by 2 and 4 dpa for ion irradiation condition for the sake of clarity.

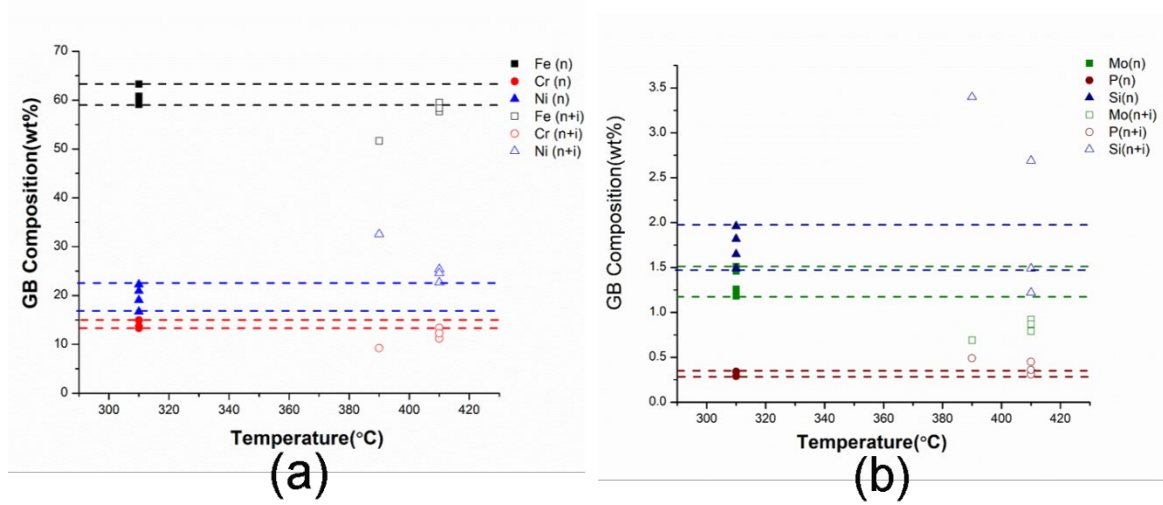


Figure 9: A direct comparison of RIS in neutron and neutron + ion irradiated samples with a similar damage level ~73dpa. (a) Major elements and (b) Minor elements. The temperature of neutron + ion irradiation indicates the experimental temperature of ion irradiation.

5. CONCLUSIONS AND FUTURE WORK

The benchmarking work of microstructural characterization on reactor-irradiated samples with different dose levels (~41, ~74, and 100dpa) was completed. Dislocation loops, nanocavities, Ni-Si clusters, and radiation-induced segregation were all observed in specimens that were in the reactor-irradiated condition. Those features showed a sign of saturation. Void swelling was generally below 0.05%, and significant swelling is not expected as the reactor continues to operate at these conditions.

Two ion irradiations were performed to determine the best condition to emulate reactor damage. Ion irradiation can generally reproduce most of the microstructural features in reactor-irradiated samples. Irradiation performed at 410°C seems to be a better temperature than 390°C for emulating reactor damage. The samples will be continuously irradiated to 100 dpa in the next phase at 410°C and will be compared with reactor-irradiated samples at the same dose. Meanwhile, the 74 dpa samples will be irradiated to 100 dpa at the same temperature to duplicate the result. One of those samples will be further irradiated to 160 dpa, which corresponds to the life extension after 100 years.